JOURNAL OF MATERIALS SCIENCE 27 (1992) 2223–2230

Preparation and performance of reactively deposited active battery plates

S. P. JIANG, C. Q. CUI, A. C. C. TSEUNG
Chemical Energy Research Centre, University of Essex, Wivenhoe Park, Colchester CO4 3SQ, UK

Reactive deposition is a novel process for producing high-surface-area and highly porous cobalt anodes. The fundamental factors affecting the macro- and microstructure of cobalt electrodes produced by reactive deposition have been studied. The discharge performance of the reactively deposited cobalt anodes is significantly better than those prepared by solid-state sintering. The porous structure of the reactively deposited cobalt electrodes shows unique characteristics of fine and coarse pore network, which enhances the efficiency and utilization of the cobalt anodes. More significantly, it is shown that the porous structure as well as the porosity of the cobalt electrodes can be controlled by monitoring the dynamic states of the $Co(OH)_2$ colloid layer at the electrode surface, i.e. the deposition parameters. Reactive deposition opens up the feasibility of controlling the porous structure of the battery plates to enhance the utilization and efficiency of the battery plates, especially in the case of high loadings.

1. Introduction

There are two main methods of producing negative battery plates: by sintering fine metal powders in a reducing atmosphere, or by the reduction of metallic salts trapped in a porous metal structure or metallic pocket. It is difficult to control the porosity, pore size and grain size of the porous metal plates by such methods. Better control of the macro- and microstructure of battery plates should lead to higher utilization and performance.

1.1. Some practical and theoretical considerations

On discharge, most of the conventional aqueous rechargeable anodes form relatively insoluble and less conducting products which grow on the surface of the individual metal grains. This has several consequences.

1. In order to achieve higher utilization of the battery plates, the plates should be porous as this would ensure that the thickness of the reaction product on each metal grain could be kept to an absolute minimum. Once the reaction product has formed on the surface of the metal grains, further reaction would require the ions to diffuse at least partially through the product film, and this dictates that the metal grain should be small.

2. Since the density of the reaction products is usually significantly lower than that of the parent metal grains, the porosity of the battery plate should be high enough to accommodate the resulting reaction products and still leave enough channels for electrolyte to diffuse through to the interior of the plate to ensure high utilization of the remaining metal grains. Table I gives the minimum theoretical porosity required for the complete utilization of some typical rechargeable anodes used in alkaline batteries.

In the case of Co and Fe, the minimum theoretical porosity required for complete utilization is $\sim 74\%$. In practice, the porosity should be higher than the theoretical minimum as there must be enough porosity for electrolyte to diffuse into the interior of the electrode to react with any unreacted metal grains. If we assume each of the metal grains perfect spheres of equal size, and that they are packed into simple cubic structures, then the packing density is 52%, i.e. 48% porous. Bearing in mind that the metal grains are not of uniform size in practice, the packing density is likely to be higher, as the smaller grains could fit into the interstices between the larger grains, rendering it even less porous. Therefore, in the preparation of porous Co or Fe electrodes by sintering [1, 2], it is necessary to incorporate pore-forming agents such as $(NH_4)_2CO_3$ to increase the porosity of the finished product to 75–80%. The situation is not completely satisfactory, as the pore-size distribution is not uniform and the Co and Fe grains undergo grain growth on sintering. In the case of cadmium anodes, the usual preparation method involves the reduction of $Co(OH)_2$ packed inside perforated nickel plated steel pockets or porous nickel structures, with high surface-carbon or graphite additions to increase the conductivity. The use of inert materials and structures adds extra weight to the battery and reduces its capacity. Therefore there is a need to devise a better method for

0022–2461

TABLE I Minimum theoretical porosity

Anode	Density ($g\ cc^{-1}$)	Atomic weight	Product	Mol. wt	Density ($g\ cc^{-1}$)	Volume expansion (%)	Theoretical porosity (%)
Co	8.9	58.93	$Co(OH)_2$	92.95	3.597	290.2	74.37
Fe	7.86	55.847	$Fe(OH)_2$	89.847	3.4	271.91	73.11
Cd	8.642	112.47	$Cd(OH)_2$	146.47	4.79	134.95	57.43

producing battery plates, which ideally should have very small grains metallurgically joined together. The porosity of the plates should be greater than the minimum theoretical porosity required.

1.2. Reactive deposition

Electrodeposition and electroforming techniques are well-known methods for producing metallic coatings and articles. However, it is not possible to produce highly porous articles by such methods. In order to produce highly porous metal deposits, oxygen may be introduced to the substrate during electrodeposition. The continuous formation of oxides and/or hydroxides during electrodeposition should interfere with the orderly build up of the metallic layers and should result in a porous metallic structure. We have named the proposed technique 'reactive deposition' [3, 4].

Reactive deposition is a novel process involving the deposition of metal in the presence of bubbling oxygen and the presence of Cl^- ions in solution. The mechanism and kinetics of the deposition process of cobalt electrodes were extensively studied using a rotating ring disc electrode in the presence of bubbling oxygen [5–7], as well as in the presence of dissolved oxygen [8–10]. In the presence of oxygen, oxygen is reduced prior to the deposition of cobalt through a four- and two-electron process in unbuffered neutral solutions.

$$O_2 + 2H_2O + 4e = 4OH^- \quad (1)$$

and

$$O_2 + H_2O + 2e = HO_2^- + OH^- \quad (2)$$

The oxygen reduction reaction leads to a considerable increase in pH value in the vicinity of the electrode surface. The nucleation potential for the deposition of cobalt is depressed to the cathodic side due to the formation of a $Co(OH)_2$ colloid layer at the electrode surface.

$$Co^{2+} + 2OH^- = Co(OH)_2 \quad (3)$$

The crystal growth of the cobalt nuclei is also affected by the formation of this $Co(OH)_2$ colloid layer around the nuclei. On the other hand, the dynamic state, i.e. the formation and breaking processes, of such a colloid layer is controlled mainly by the oxidation of $Co(OH)_2$ by peroxide ions and by the gas sparging effect of bubbling oxygen.

$$Co(OH)_2 + HO_2^- = CoOOH + 2OH^- \quad (4)$$

$$3CoOOH + HO_2^- + H_2O = Co_3O_4{\cdot}H_2O + 4OH^- \quad (5)$$

As a result, Co^{2+} ions are most easily deposited through the open channels on the $Co(OH)_2$ colloid layer, created either by the oxidation of H_2O_2 or by the sparging effect of the bubbling oxygen. In other words, the nucleation and crystal-growth processes of cobalt are localized in the presence of oxygen. The deposition of cobalt probably takes place at the sites where cobalt hydroxide/oxide are reduced and precipitated.

$$Co^{2+} + 2e = Co \quad (6)$$

$$CoOOH + H_2O + 3e = Co + 3OH^- \quad (7)$$

$$Co_3O_4 + 4H_2O + 8e = 3Co + 8OH^- \quad (8)$$

Such localized deposition processes are responsible for the high-surface-area and highly porous structure of the cobalt electrodes obtained by reactive deposition. It has been found that the efficiency of the dynamic states of the $Co(OH)_2$ colloid layer on the porous structure of the electrodes deposited is directly related to the nature of the electrochemical system [8, 9].

So far, our work has concentrated on the reactive deposition of porous cobalt. In this paper, the deposition process of porous cobalt anodes is reported, and the factors which control the porosity as well as the porous structure will be discussed. Future work on the optimization of the porous structure in order to maintain the high utilization of the cobalt electrodes in the case of high cobalt loadings will be outlined.

2. Experimental procedure

Reactive deposition of cobalt was carried out in an electrolyte cell as described previously [5]. Gas (oxygen or air or nitrogen) was fed through a sintered glass plug directed onto the working electrode. The flow rate of gases was generally controlled at 200 ml min^{-1}. Cobalt electrodes were galvanostatically deposited in 0.25 M $CoCl_2$ at 20 mA cm^{-2} and 25 °C for 1 h under an oxygen flow of 200 ml min^{-1}. The deposition potential was measured against a saturated calomel electrode (SCE) reference electrode (BDH, Pook). The morphology of cobalt electrodes was examined by scanning electron microscopy (SEM).

A nickel screen (60 mesh) was used as the metal substrate in this study. The nickel screen was thoroughly washed with washing liquid, diluted HCl solution and diluted KOH solution. Each step was followed by ultrasonic treatment for about 15 min. The Ni substrates were then washed with distilled water and dried at 60 °C. The apparent surface area of the Ni substrates was 1 cm^2 (counting one side only). Cobalt metal (99.5% Co, supplied by Cobalt Development Institute, London) was used as the counter electrode. The electrolyte was made from various

cobalt salts and distilled de-ionized water. In general, the concentration of the solution was 0.25 M. The loading of the cobalt deposited was determined by a visible spectroscopy method. The theoretical capacity of the Co electrodes was then calculated (based on 0.909 Ah g^{-1}). The current setting for the steady-state discharge/charge of the electrodes was obtained by dividing the theoretical capacity (C) by the period of interest (h) for a given C rate.

The electrode performance was studied in 7 N KOH solution at room temperature. The voltammetric curves and the charge/discharge performance of the electrodes were examined at various conditions. The potential was measured against an Hg/HgO reference electrode. Voltammetry was performed in a potential range of -1.1 to $+0.5$ V (against Hg/HgO). A platinum screen was used as the counter electrode.

3. Results and discussion

3.1. Porous structure of reactivity deposited cobalt electrodes

Cobalt electrodes were deposited from a 0.25 M $CoCl_2$ solution at 20 mA cm^{-2}, 25 °C for 1 h in the presence of bubbling O_2 and N_2. The deposited specimens in the presence of bubbling N_2 were grey in colour, while the specimens prepared in the presence of bubbling O_2 were black. Fig. 1 shows SEM of the cobalt deposited under bubbling various gases.

Cobalt deposited in the absence of oxygen (Fig. 1a) shows the typical structure of an electrodeposited layer, i.e. metallic grains tightly packed together. The large crystals of the deposits indicate the increased mass-transfer process of Co^{2+} ions in the presence of bubbling N_2 as in the case of gas sparging where bubbling nitrogen is used [11, 12]. On the other hand, cobalt deposited in the presence of bubbling oxygen shows very fine Co grains ($\sim$ 0.5 μm) with fine pores ($\sim$ 0.2–0.5 μm) and coarse pores ($\sim$ 2 μm) between them (Fig. 1b). These Co grains are joined together metallurgically, resulting in a significantly high conductivity. The interlaced network of fine and coarse pores, and the high conductivity of the Co electrodes, are confirmed by their higher performance for the evolution of H_2 and O_2 in alkaline solutions as compared to Teflon-bonded electrodes [13]. After discharge (100 mA cm^{-2}, 15 h), hexagonal cobalt hydroxide/oxide grains are intimately interwoven together (Fig. 1c). However, the unique porous structure of fine and coarse pores produced by reactive deposition still remains. Fig. 1d also shows the porous structure of Co anodes produced by powder metallurgical techniques (750 °C, hydrogen, 25 wt % ammonium carbonate was added as pore forming agent, 1 h [1]. The cobalt grains are very much larger ($\sim$ 5 μm) than those prepared by reactive deposition ($\sim$ 0.5 μm). In addition, the pores are non-uniform, i.e. large pores from the inclusion of the ammonium carbonate pore former, and small pores between the cobalt grains.

3.2. General performance of electrodes

Fig. 2 shows typical potential sweep curves of a newly prepared Co electrode with various reversal poten-

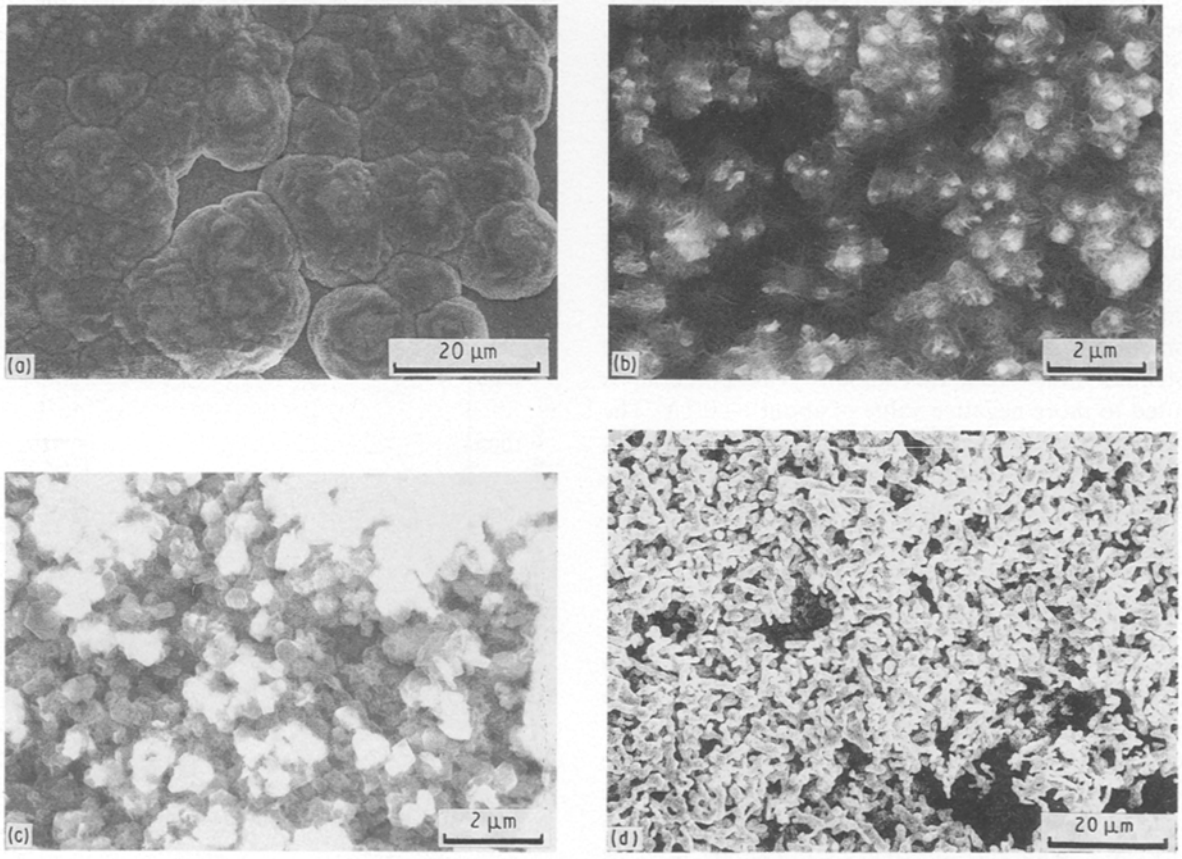

Figure 1 Electron micrographs of Co electrodes prepared using various methods: (a) in presence of bubbling N_2; (b) bubbling O_2; (c) reactively deposited Co anode, after evolving O_2 for 15 h at 100 mA cm^{-2}, 7 N KOH, RT; (d) sintered Co anode (750 °C, H_2, 25% $(NH_4)_2CO_3$ added).

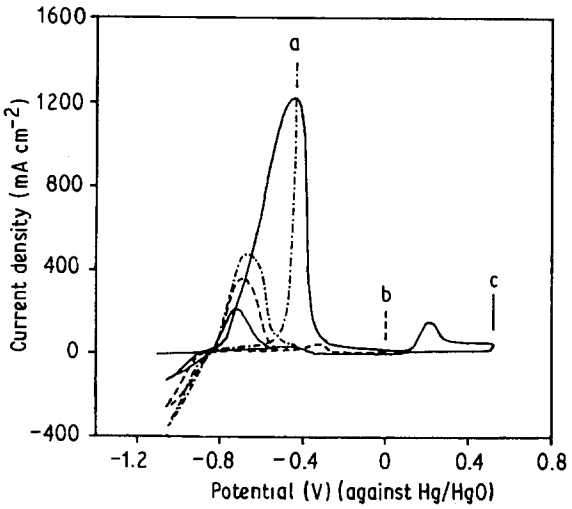

Figure 2 Cyclic voltammetric curves of a reactively deposited Co electrode in 7 N KOH at scan rate of 10 mV s^{-1}. Letters indicate position of reversal potentials.

tials at scanning rate of 10 mV s^{-1}. The cobalt electrode was reactively deposited in 0.25 M $CoCl_2$ at 20 mA cm^{-2} for 1 h. The electrode was completely charged at − 1.1 V before the test. In the potential range of − 1.1 to + 0.5 V (against Hg/HgO), there are two distinct anodic peaks, a large one at about − 0.45 V and a much smaller one at + 0.3 V, respectively. The first oxidation peak in the voltammograms occurs at about − 0.85 V and rises rapidly from about − 0.75 V. The rising portion of this peak is due to the thickening of the cobaltous hydroxide film along with the formation of less soluble cobalt oxide. The calculated potentials for the electrode couples $Co/Co(OH)_2$ and Co/CoO are − 0.818 and − 0.792 V, respectively [14]. The second one at about + 0.3 V corresponds to the reaction of $Co(OH)_2$ or CoO/CoOOH. The sharp decrease of the anodic current after the anodic peak potential is due to the passivation of the electrodes.

The cyclic voltammograms at different reversal potentials show that the first anodic peak current of the second successive potential scan is much smaller than that of the first potential scan, even though this oxidation current increases with the decreasing upper scan potential limit. Also, this anodic peak potential is shifted to more negative value of about − 0.7 V. The sharp decrease of this first oxidation peak current shows that the amount of the reduced cobalt hydroxide/cobalt oxides during successive cathodic scan is very small. This indicates that the cobalt hydroxide/oxides, especially at the electrode surface formed during oxidation, could block the pores of the electrode and increase the diffusion polarization. Further reduction of the inner layer of the $Co(OH)_2$ or CoO becomes relatively difficult. However, the electrode performance can be totally recovered after the complete charging of the electrode at − 1.10 V. Therefore the anodic peak current density, i_{ap}, and the discharge capacity integrated in a potential range of − 1.1 to 0.0 V at a scan rate of 10 mV s^{-1} can be used as parameters to compare the anodic performance of the electrodes prepared at various conditions.

3.3. Effect of bubbling gases

Fig. 3 shows the effect of different gases on the anodic peak current density of the cobalt electrodes deposited at 20 mA cm^{-2} for 1 h at 0.25 M $CoCl_2$. It shows that the anodic performance of the Co electrodes deposited in the absence of O_2 and in the presence of bubbling N_2 is very low. Bubbling air onto the metal substrate during electrodeposition considerably increased the i_{ap} value. In the presence of bubbling O_2, the anodic peak current density increases to more than 1000 mA cm^{-2}. The fact that bubbling N_2 does not result in the increase of the anodic performance confirms that the formation of the porous deposits is not due to the sparging effect of the bubbling gases. In contrast, the sparging effect of bubbling nitrogen is to increase the mass transfer process as indicated by Fig. 1a. The formation of high-surface-area and highly porous cobalt structure is due to the localized nucleation and crystal growth process of Co^{2+} ions in the presence of bubbling oxygen (reactions [1–8]).

3.4. Effect of anions of cobalt solutions

The anodic performance of the cobalt electrodes deposited in the presence of bubbling oxygen is greatly affected by the anions in the cobalt solution. Fig. 4 compares the anodic peak current densities of the electrodes deposited at 20 mA cm^{-2} for 1 h in 0.25 M $CoCl_2$, 0.25 M $CoSO_4$, 0.25 M $(CH_3COO)_2Co$, and 0.25 M $Co(NO_3)_2$ solutions, respectively. The cobalt electrode prepared in $CoCl_2$ solution gave the best results.

In the study of oxygen reduction in unbuffered neutral solutions, it has been found that the mechanism and kinetics of oxygen are directly related to the anions in the solutions [6, 8]. In the presence of Cl^- ions, a parallel mechanism of four- and two-electron processes is found for oxygen reduction with formation of about 31% H_2O_2, as compared to about 9% H_2O_2 in sulphate solutions. In the presence of buffering agents such as CH_3COO^- ions, oxygen is reduced mainly through the four-electron process to form water, as little peroxide is detected [8, 15]. In

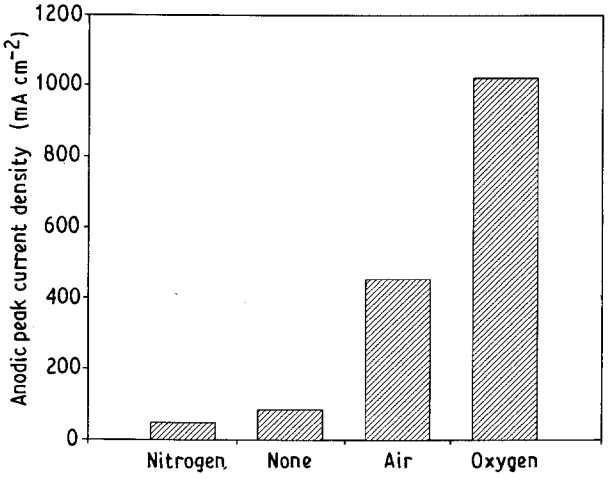

Figure 3 Effect of bubbling gases (200 ml min^{-1}) on anodic peak current density of reactively deposited Co electrodes (Co loading: 22 mg cm^{-2}) in 7 N KOH, RT.

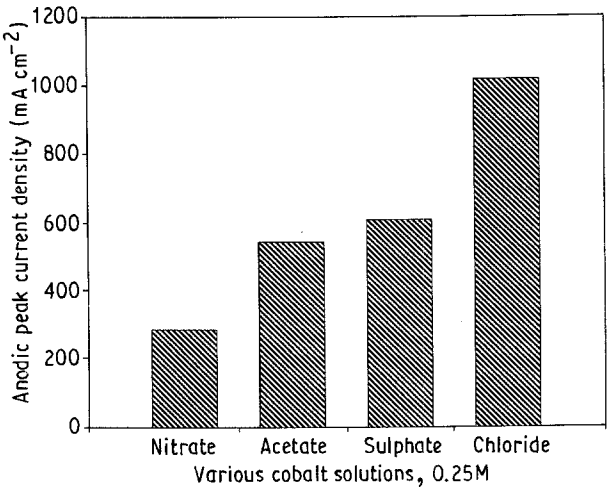

Figure 4 Effect of anions in cobalt solutions (0.25 M) on anodic peak current density of reactively deposited Co electrodes (Co loading: 22 mg cm^{-2}) in 7 N KOH, RT.

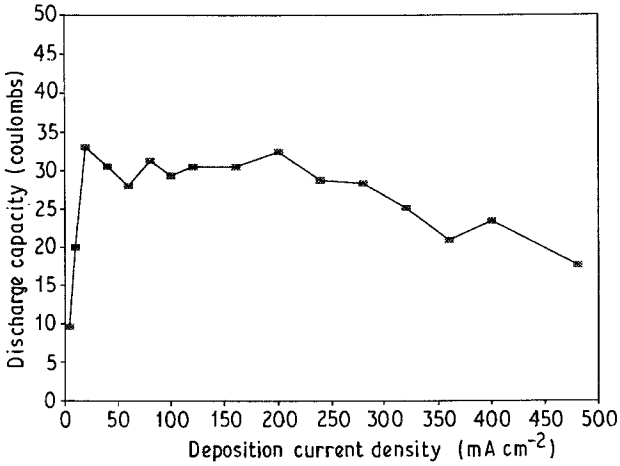

Figure 5 Effect of deposition current density at a constant deposition capacity of 72 coulombs on discharge capacity of reactively deposited Co electrodes in 7 N KOH, RT.

cobalt solutions, the $Co(OH)_2$ colloid layer is formed at the electrode surface as the result of the preceding oxygen reduction. On the other hand, some of the $Co(OH)_2$ colloids can be oxidized by H_2O_2 to form various cobalt oxides in the presence of Cl^- ions, resulting in the thinning and breaking of the $Co(OH)_2$ colloid layer in addition to the sparging effect of bubbling oxygen. In the presence of $SO_4^=$ ions, the effect of oxidation of H_2O_2 on the dynamic states of the $Co(OH)_2$ colloid layer is negligible, which is especially true in the case of buffered solutions (for example in the presence of acetate ions). The $Co(OH)_2$ colloid layer could only be broken by the sparging effect of the bubbling gas. This will result in significant difference in macro- and microstructures of the electrodes [7].

It has been found by SEM [7] that in 0.25 M $CoSO_4$ solution, the deposits are grown in the shape of bamboo. Cobalt grains are relatively larger (~ 2–3 μm) with similar sized pores between them, as compared to those formed in $CoCl_2$ solutions. This significantly reduces the porosity of the electrode as shown by its lower anodic performance (Fig. 4). On the other hand, dense layers have been observed from the deposits obtained from $Co(NO_3)_2$ and $(CH_3COO)_2Co$ solutions. As the porosity of the electrodes in these cases could be well below the theoretical minimum value, the efficient transfer of the electrolyte for the electrochemical reactions becomes difficult, resulting in loss of efficiency and utilization of the electrodes. It has been found that the reversibility of the electrodes deposited from cobalt nitrate and cobalt acetate solutions is very poor, even after charging the electrode at − 1.10 V (against Hg/HgO) for quite a long time. This could be due to blocking of the micropores in the electrode surface.

3.5. Effect of deposition current density

Fig. 5 shows the effect of the deposition current density on the discharge capacity of the Co electrodes deposited in a 0.25 M $CoCl_2$ at a constant deposition capacity of 72 Coulombs. At low range of deposition current density (< 20 mA cm^{-2}), the discharge capacity of the electrodes deposited is relatively lower, indicating the lower porosity of the electrodes. The reason is the dominance of the interfacial electron transfer process, which limits the role of the $Co(OH)_2$ colloid layer on the kinetics of deposition process of cobalt [9]. As deposition current density is higher than 300 mA cm^{-2}, the discharge capacity is also subsequently decreased. This is due to the fact that the kinetics of cobalt deposition is mainly controlled by the mass transfer process. In such circumstances, the effects of the dynamic states of the $Co(OH)_2$ colloid layer on the kinetics of nucleation and crystal growth processes of cobalt are largely reduced. The growth of dendritic deposits was also observed at high deposition current densities.

3.6. Effect of concentration of cobalt chloride solutions

The effect of the concentration of cobalt chloride solutions on the electrochemical performance of the deposited electrodes was found to be the same as the effect of the deposition current density. Fig. 6 shows the discharge capacities of the cobalt electrodes (Co loading: 22 mg cm^{-2}) deposited at various concentrations of Co^{2+} ions. Clearly, the highest discharge capacity of the electrode is the one prepared in the concentration of 0.25 M $CoCl_2$. As the cobalt concentration is reduced, the corresponding discharge capacity is also decreased. More remarkably, the anodic performance of the electrodes decreases sharply as the cobalt concentration is higher than 0.25 M. In the case of 0.5 M $CoCl_2$, the anodic performance of the electrode is almost the same as that prepared in the absence of bubbling oxygen. This shows that at high concentration of the Co^{2+} ions, the electron transfer process for the reduction of Co^{2+} ions becomes increasingly predominant and, consequently, the inhibiting effect of the $Co(OH)_2$ colloid layer at the electrode surface is correspondingly decreased, as in the case of low-deposition current density.

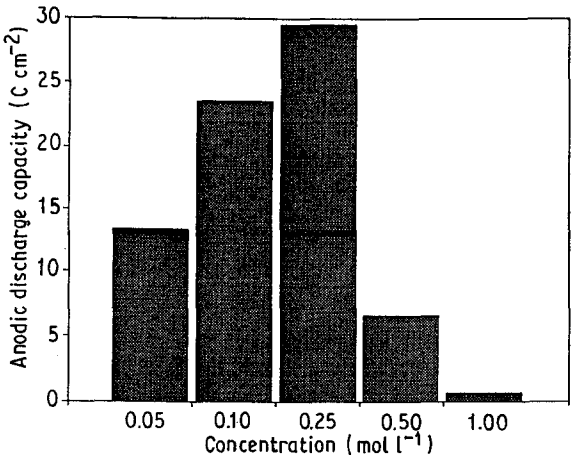

Figure 6 Effect of concentration of Co^{2+} ions on discharge capacity of reactively deposited Co electrodes (Co loading: 22 mg cm^{-2}).

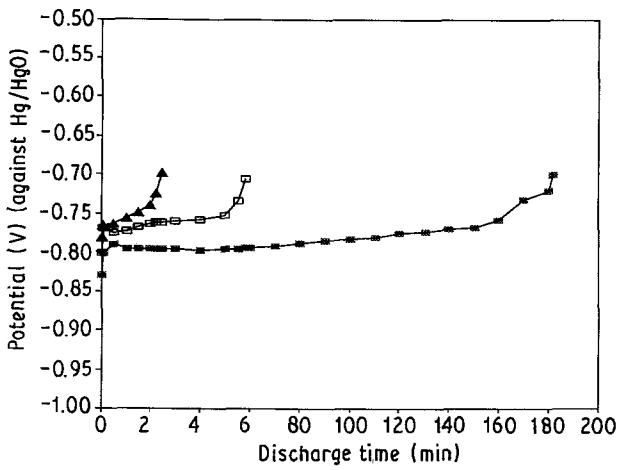

Figure 7 Discharge curves of a reactively deposited Co electrode (Co loading: 22 mg cm^{-2}) in 7 N KOH at various C rates: ■, $C/4$; □, $C/1.4$; ▲, $C/1$.

3.7. Discharge performance of cobalt electrodes

Fig. 7 represents the anodic performance of a reactively deposited Co electrode (36 mg cm^{-2}) in 7 N KOH at various C rates. At $C/4$, the depth of discharge of the reactively deposited Co electrode was about 75%. In the case of sintered Co electrodes, the depth of discharge at $C/5$ is generally in the range of 30–40% [1]. Fig. 8 compares the depth of discharge values of the reactively deposited Co electrodes with different Co loadings. It shows that at higher loadings (72 mg cm^{-2}), the depth of discharge of the electrode is about 74% at $C/4$. The utilization efficiency of the reactively deposited cobalt electrodes remains unchanged despite the increase of the Co loading. This indicates that the structure produced by reactive deposition is highly porous not only on the surface, but also in the internal layers of the electrodes.

Fig. 9 compares the discharge performance of a reactively deposited Co electrode (Co loading: 154 mg cm^{-2}) and a sintered Co electrode (Co loading: 500 mg cm^{-2}). The sintered cobalt electrode was prepared by sintering at 750 °C for 1 h with addition of 25% $(NH_4)_2CO_3$ [1]. The polarization performance of the electrode was measured at scan rate of 2.4 mV s^{-1}. The anodic current density of the cobalt electrode prepared by reactive deposition is as high as 1100 mA cm^{-2} at an anodic potential of − 0.6 V (against Hg/HgO) as compared to about 300 mA cm^{-2} for the sintered cobalt electrode at the same discharge conditions, even though the Co loading of the sintered electrode is three times higher than that of the reactively deposited Co electrode. It is clear that the reactively deposited Co electrode shows much higher activity than that of the sintered Co electrodes.

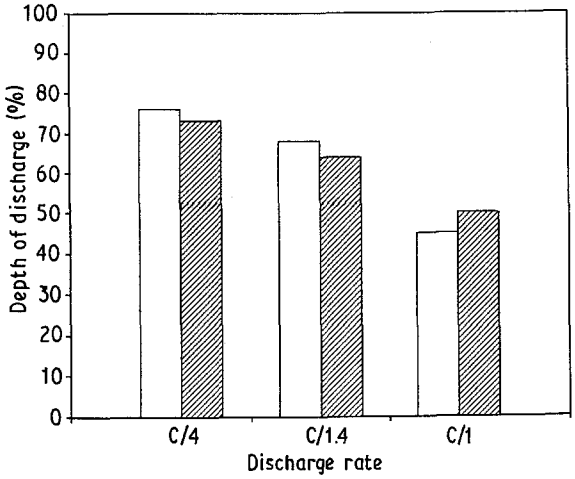

Figure 8 Depth of discharge of reactively deposited Co electrodes with different Co loadings as a function of C rates. □, 36; ▨, 72 mg.

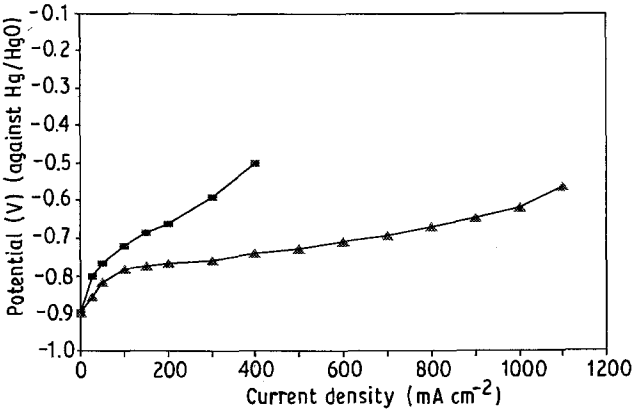

Figure 9 Comparison of anodic performance of ▲, a reactively deposited Co electrode (Co loading: 154 mg cm^{-2}) and ■, a sintered Co electrode (Co loading: 486 mg cm^{-2}) measured in 7 N KOH at scan rate of 2.4 mV s^{-1}.

3.8. Control of porosity and porous structure of Co electrodes

Control of the porous structure as well as the porosity of the electrodes is very important, especially in the case of high loadings. In theory, the minimum porosity required for the complete utilization of a Co electrode is ~ 74%. In the case of a reactively deposited Co electrode, it has been found that the discharge capacity measured at very low discharge rate ($C/200$) was almost the same as the theoretical discharge capacity. This shows that the porosity of the reactively deposited Co electrode is at least ~ 74%.

In the case of the reactive deposition, the porous structure of the electrodes is mainly controlled by the mechanism and kinetics of the localized nucleation and crystal-growth processes of Co^{2+} ions, which in turn are greatly dependent on the dynamic states of the $Co(OH)_2$ colloid layer formed at the electrode surface. Fig. 10 shows the porous structure of Co electrodes deposited in a 0.25 M $CoCl_2$ solution and in the presence of dissolved O_2 and of bubbling air. In the presence of dissolved rather than bubbling oxygen, large Co grains and pores are observed (Fig. 10a). The porous structure prepared in the presence of dissolved O_2 is very different from that prepared in the presence of bubbling O_2 (Fig. 1b). This can be explained by the fact that in the presence of dissolved O_2, the $Co(OH)_2$ colloid layer can only be partially thinned and broken by the oxidation reaction of $Co(OH)_2$ by H_2O_2 (reaction [4, 5]). This compares to the case of the presence of bubbling O_2, where the dynamic states of the $Co(OH)_2$ colloid layer are also greatly affected by gas sparging. The limited breaking process of the $Co(OH)_2$ colloid layer in the presence of dissolved oxygen retards the formation and growth of cobalt nuclei. In turn, the rate for the crystal growth process could be increased due to the limited nucleation reaction, especially in the circumstances at which the height of the cobalt grains exceeds the thickness of the colloid layer. This could be the reason for the formation of relatively large bamboo-shaped cobalt crystals ($\sim$ 2–4 μm) in the vertical direction (Fig. 10a). For the same reason, bubbling air instead of bubbling oxygen reduces the activity of the oxygen reduction, resulting

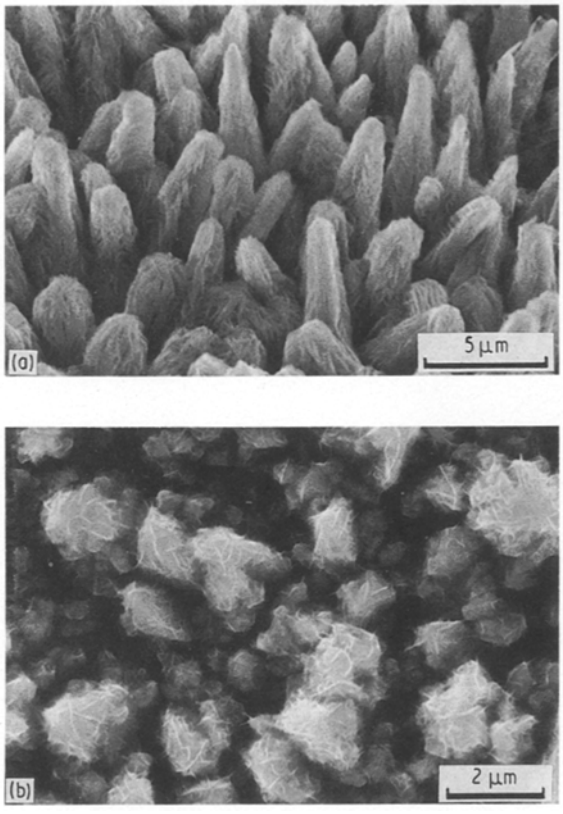

Figure 10 Porous structure of Co electrodes deposited in 0.25 M $CoCl_2$ at 20 mA cm^{-2} for 1 h in the presence of dissolved O_2 and bubbling air.

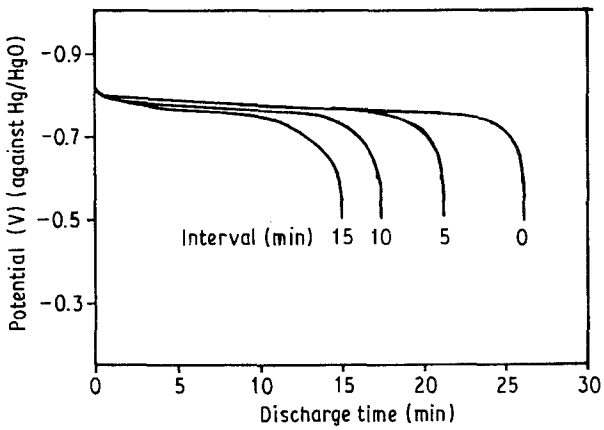

Figure 11 Discharge curves of reactively deposited Co electrodes in 7 N KOH at $C/1$. The electrodes were deposited by switching on and off the bubbling O_2 at various intervals.

in the decrease of the formation of peroxide and the thickness of the $Co(OH)_2$ colloid layer. Consequently, it would be expected that the porous structure of the cobalt electrode prepared in the presence of bubbling air will have relatively large Co grains and pores, as compared to that in the case of bubbling oxygen. This is shown to be the case by the morphology of the cobalt electrode deposited in the presence of bubbling air (Fig. 10b).

The porous structure obtained in the presence of dissolved O_2 and of bubbling air opens up the possibility of controlling the porous structure as well as porosity of the Co electrodes through control of the deposition parameters. An example is given in Fig. 11, where the electrodes (Co loading: 22 mg cm^{-2}) were deposited in a 0.25 M $CoCl_2$ solution by switching on and off the bubbling O_2 at various intervals. The discharge curves were measured in 7 N KOH at $C/1$. The utilization efficiency of the electrodes increases with the decrease in the time between bubbling of oxygen and its cessation (i.e. deposition in the presence of dissolved oxygen), indicating that the porosity of the electrode has been increased. This approach opens the way for better control of the porosity and grain structure of cobalt electrodes, and could be particularly advantageous in the case of high-loading electrodes. Preliminary work on the reactive deposition of Fe, Cd and NiOOH has also yielded encouraging results [3].

4. Conclusions

Reactive deposition is a novel process for producing high-surface-area and highly porous cobalt anodes. The fundamental factors affecting the macro- and microstructure of cobalt electrodes produced by reactive deposition have been studied, and their performance is significantly better than those prepared by solid-state sintering. The porous structure of the reactively deposited cobalt electrodes shows unique characteristics, of fine and coarse pore networks, which improve the efficiency and utilization of the cobalt anodes. Reactive deposited Fe, Cd and NiOOH gave significant improvements in performance over conventionally prepared battery plates.

More significantly, mechanistic studies on the deposition process of cobalt [4–10] have shown that the kinetics of the deposition process of cobalt in the presence of oxygen are characterized by the localized nucleation and crystal growth processes of cobalt. This in turn is dependent on the dynamic state of the $Co(OH)_2$ colloid layer formed at the electrode surface. It has been shown that the porous structure as well as the porosity of the cobalt electrodes can be controlled by monitoring the dynamic states of the $Co(OH)_2$ colloid layer at the electrode surface. Reactive deposition shows the feasibility of controlling the porous structure of the battery plates to enhance the utilization and efficiency of the battery plates, especially in the case of high loadings.

Acknowledgements

C.Q.C. was in receipt of a Sino-British Friendship Scholarship. The work was also supported by the City University, Mineral Industries Research Organization and the Academic Link Programme with China, British Council.

References

1. T. S. K. TANG, PhD Thesis, The City University, London (1986).
2. P. R. VASSIE and A. C. C. TSEUNG, *Electrochim. Acta* **21** (1966) 299.
3. A. C. C. TSEUNG, S. P. JIANG, Y. Z. CHEN and J. K. YOU (1988) British Provisional Patent Application No. 88 154 943, (June 1988).
4. *Idem., J. Mater. Sci. Lett.* **9** (1990) 1294.
5. S. P. JIANG, Y. Z. CHEN, J. K. YOU, T. X. CHEN and A. C. C. TSEUNG, *J. Electrochem. Soc.* **137** (1990) 3374.
6. S. P. JIANG and A. C. C. TSEUNG, *ibid.* **137** (1990) 3381.
7. *Idem., ibid.* **137** (1990) 3387.
8. S. P. JIANG, C. Q. CUI and A. C. C. TSEUNG, *ibid.* **137** (1990) 3418.
9. C. Q. CUI, S. P. JIANG and A. C. C. TSEUNG, *ibid.* **138** (1991) 94.
10. *Idem., ibid.* **138** (1991) 1086.
11. W. COOPER and K. MISHRA, *Hydrometallurgy* **17** (1985) 305.
12. D. A. UCEDA and T. J. O'KEEFE, *J. Appl. Electrochem.* **20** (1990) 327.
13. S. P. JIANG and A. C. C. TSEUNG, *J. Electrochem. Soc.* **138** (1991) 1216.
14. W. K. BEHL and J. E. TONI, *J. Electroanal. Chem.* **31** (1971) 63.
15. V. JOVANCICEVIC and J. O'M. BOCKRIS, *J. Electrochem. Soc.* **133** (1986) 1797.

Received 7 January
and accepted 25 March 1991